Theoretical Characterizations of Spinels Containing Iron and Vanadium *via ab initio* Calculations

Jianping XIAO,[1,2,3]* Bing XIE[1] and Yu WANG[1]

1) College of Materials Science and Engineering, Chongqing University, Chongqing, 400030 China.
2) Bremen Center for Computational Materials Science, Universität Bremen, Am Fallturm 1, Bremen, 28359 Germany.
3) School of Engineering and Science, Jacobs University Bremen, Campus Ring 1, Bremen, 28759 Germany.

We have employed *ab initio* approaches to investigate normal and inverse spinels containing iron and vanadium. The valence states of tetrahedral and octahedral Fe and V were firstly calibrated with reference oxides FeO (rocksalt), Fe_2O_3 (corundum), VO (rocksalt) and Fe_2O_3 (corundum). The Mulliken charges analyses suggest the valence states of Fe and V are interstices dependent. In Fe rich condition (VFe_2O_4), bivalent cations Fe^{2+} and V^{2+} prefer tetrahedral interstices, while trivalent cations Fe^{3+} and V^{3+} prefer octahedral interstices. In V rich condition (FeV_2O_4), Fe valence states in tetrahedral and octahedral interstices are the same as those in Fe rich cases. However, the V cations have contrary valence states, namely, V^{3+}, in tetrahedral interstices, and mixed valence states in octahedral states.

The crystalline formation energies of normal and inverse spinels were addressed to determine their stability. The inverse spinels are obviously more favorable than normal spinels. We have quantified probability of two isomeric inverse spinels in Fe rich condition in equilibrium at 300 K and 1 700 K. It is in agreement with that entropy plays a more significant role at high temperature. Electronic structures of tetrahedral and octahedral Fe and V cations have also been analyzed using computed x-ray absorption near edge structure (XANES). The chemical shift of white lines, going from Fe^{2+} to Fe^{3+} cations in spinels, and $3d$ orbitals splitting of tetrahedral and octahedral V cations are distinguishable in XANES spectra. Thus, the different electronic structure of Fe and V cations in tetrahedral and octahedral interstices can provide important interpretations of experimental works of spinels containing iron and vanadium elements.

KEY WORDS: vanadium; spinel; valence state; formation energy; *ab initio* calculations.

1. Introduction

Metallic vanadium is an important alloying ingredient to produce ferrovanadium and advanced tool steels in iron-steel industry.[1] Industrial production of vanadium includes two main consecutive processes. Firstly smelting vanadium containing slag can be produced using converter in pyrometallurgical processes and be cooled down to solid state at ambient condition. Then the solid state vanadium containing slag is utilized to extract vanadium in hydrometallurgical processes.[2] Thus, the vanadium containing slag is critical intermediate media for industrial vanadium production. As it is a chemical process in Fe rich condition in converter, the vanadium-iron spinels, namely, VFe_2O_4, are dominant compounds in vanadium containing slag. Furthermore, vanadium-iron spinel is also a very promising compound due to its interesting properties in magnetic, magnetooptical[3] and electrical transport.[4] However, the Fe and V with variational valence states can form complicated and multiform $[Fe,V]_T[Fe,V]_OO_4$ spinels, where subscripts T and O indicate tetrahedral and octahedral interstices, respectively. In normal spinel structures, the identical elements (Fe and V) always occupy equivalent tetrahedral or octahedral coordination interstices, while the same elements (Fe and V) can be present with mixed coordination in inverse spinel structures. Since the normal and inverse spinels have identical space group (Fd-3m) and similar lattice constant,[5,6] they usually coexist in the form of solid solutions. Thus, quantitive characterization of normal and inverse vanadium-iron spinels is extremely difficult, *e.g.*, valence states, stability and isomeric fractions. Therefore, theoretical investigations are of significant roles in characterizing solid solution systems.

The quantitive characterization requires accurate evaluations of crystalline formation energies. *Ab initio* approaches calculate energies and charge transfer quantum mechanically, which is more accurate than classical models and semi-empirical methods. It is quite effective to investigate variational valence systems, *e.g.* transition metal elements Fe and V. Recently, Chung *et al.*[7] had successfully addressed interface energies of solid transition metal carbides (V, Nb and Ta) and bcc iron *via ab initio* studies. Guthrie *et al.*[8] had also predicted interfacial thermal effects by *ab initio* mathematical models. The *ab initio* calculations fail to address strong electronic correlation matters due to its local density approximations (LDA). Recently advanced hybrid functionals were developed and can reproduce successfully experimental

observations of strong electronic correlation systems.

In this work, we have employed hybrid functional to study formation energies of normal and inverse spinels containing iron and vanadium. The probability of bivalent and trivalent Fe and V cations in Fe-rich condition has been evaluated by analyzing thermal vibrational contributions, for spinel systems with thermodynamic equilibrium state. The electronic structures are analyzed with computed X-ray absorption near edge structure (XANES) to provide interpretations for experimental characterization for realistic spinel systems in nonequilibrium.

2. Computational Models and Methodology

The mixed-metal oxide spinel can be regarded as a closely cubic packed anion (oxygen) with 1/8 tetrahedral and 1/2 octahedral cation occupations. The remainder 7/8 tetrahedral interstices and 1/2 octahedral interstices are unoccupied.[9] All studied spinel structures containing iron and vanadium are described by our computational models, represented in **Fig. 1**, in the view of periodic primitive cell. In V rich condition, the 1/8 tetrahedral interstices are occupied by Fe cations and 1/2 octahedral interstices by V cations in normal spinel (Fig. 1(a)). In contrast, the V cations occupy 1/2 octahedral interstices and the Fe cations pack at 1/8 tetrahedral interstices in normal spinel in Fe rich condition (Fig. 1(d)). Due to a half of cations exchange packing position, it induces inverse spinel structures in both Fe and V condition (Figs. 1(b), 1(c), 1(e) and 1(f)). The favorable packing of metallic cations depends on their crystal field stabilization energies (CFSE). Thus, we have also studied various mixed occupations of Fe and V cations on octahedral interstices in reverse spinel structures.

The *ab initio* calculations were carried out with quantum mechanical program CRYSTAL09.[10] To obtain comparable energies, we have specified equivalent $4 \times 4 \times 4$ space grids in irreducible Brillouin zone of the reciprocal space with Monkhorst-Pack scheme.[11] Validated local Gaussian-type basis functionals were employed with all-electron considerations in order to be independent of parameterizations of

pseudopotentials (Fe: 86-411(41d),[12] V: 86-411(4d)[13] and O: 6-31(1d)).[14] We have validated that spin induced energetic difference of normal and inverse spinel systems is smaller than the magnitude of formation energies. Thus, we have assigned ferromagnetic spin ordering for all systems and do not discuss other spin configurations in this work. Both lattice parameters and internal coordinates were relaxed to obtain energetic minimum. The reliable accuracy can be achieved with around 2% and 3% underestimation of lattice constant (**Table 1**) for normal and inverse spinel structure.[5,6] For calibration of bivalent and trivalent Fe and V cations, we have employed the following oxide phases, namely, FeO (rockslat), Fe_2O_3 (corundum), VO (rockslat) and V_2O_3 (corundum), on the basis of Mulliken charge population analyses. The thermal contributions of lattice vibration were also analyzed using *ab initio* calculations to quantify spinels systems in thermodynamically equilibrium. The XANES calculations were performed based on FEFF9.0 code[15] to interpret crystal field splitting of $3d$ orbitals of tetrahedral and octahedral Fe and V cations. As the electronic structures of Fe and V cation in tetrahedral and octahedral interstices are distinguishable, the computed XANES can advise and interpret experimental characterizations.

To compare stability of spinels, we need to calculate formation energies of spinels. The referred valence states of Fe and V are quite critical. Therefore, we first calibrated interstices dependence of valence states in normal and inverse spinels structures *via* Mulliken charge analyses. The computed Mulliken charges of normal and inverse spinel structure are listed in **Table 2**. The Mulliken charges of tetrahedral Fe
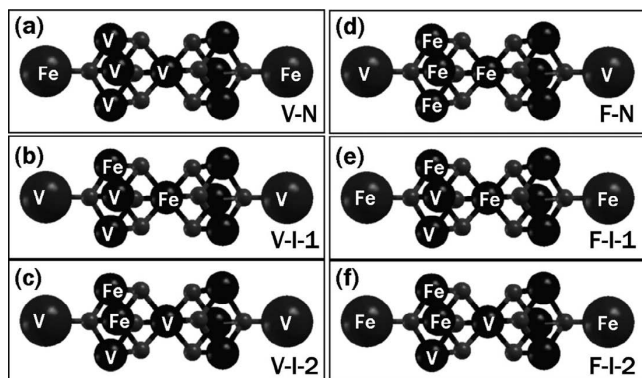

Fig. 1. Atomistic arrangements of normal and inverse spinel structures, in view of periodic primitive cell, are illustrated schematically. The smallest, moderate and largest spheres describe anionic interstices, octahedral and tetrahedral cation interstices, respectively. (a), (b) and (c) are normal and inverse spinel structures in V-rich condition; (d), (e) and (f) are normal and inverse spinel structures in Fe-rich condition, respectively.

Table 1. Computed lattice constant, *a*, of normal and inverse spinel structures are compared with experimental observations (Å).

Functionals	VBH	PBE	B3LYP	PBE0	exp.
V-N	8.139	8.331	8.349	8.303	8.543 [6]
V-I-1	8.096	8.254	8.431	8.375	–
V-I-2	8.083	8.249	8.431	8.375	–
F-N	8.308	8.494	8.100	8.433	–
F-I-1	8.047	8.229	8.298	8.247	8.297 [5]
F-I-2	8.047	8.229	8.298	8.247	8.297 [5]

Table 2. Valence states of Fe and V were calibrated in terms of comparisons between Mulliken charges of reference compounds and those of all studied spinel structures. The subscripts T and O are used to describe tetrahedral and octahedral interstices.

	$Fe^{2+}(FeO)$	$Fe^{3+}(Fe_2O_3)$	$V^{2+}(VO)$	$V^{3+}(V_2O_3)$
Mulliken Charges	+1.54	+2.06	+1.53	+1.93
	Fe_T	Fe_O	V_T	V_O
V-N	+1.65	–	–	+1.92
V-I-1	–	+2.06	+1.86	+1.60
V-I-2	–	+2.06	+1.86	+1.60
F-N	–	+2.06	+1.57	-
F-I-1	+1.66	+2.05	–	+1.95
F-I-2	+1.66	+2.05	–	+1.94

cation of V-N, F-I-1 and F-I-2 spinels are almost equal to Fe^{2+} reference in the phase of rocksalt FeO. Also the Mulliken charge of the corundum Fe_2O_3 is close to octahedral Fe cation. Thus, the Fe^{2+} cations prefer to occupy tetrahedral interstices in studied spinels, while Fe^{3+} cations prefer only octahedral interstices. However, the valence states of V cations are significantly different. In the cases of V-N, F-I-1 and F-I-2, the V cations have consistent interstices dependence compared with that of Fe cations, while there are inverse chemical states for V-I-1 and V-I-2 cases, that is, the V^{2+} cations prefer to locate at octahedral interstices and V^{3+} in tetrahedron.

3. Results and Discussion

3.1. Quantifications in Equilibrium

According to above discussion, formation energies calculations of normal FeV_2O_4 and VFe_2O_4 spinels structures were referred to $2[Fe]_T^{2+}4[V]_O^{3+}$ and $2[V]_T^{2+}4[Fe]_O^{3+}$ with chemical composition of $2FeO\cdot2V_2O_3$ and $2VO\cdot2Fe_2O_3$, respectively. Furthermore, the inverse FeV_2O_4 and VFe_2O_4 spinels structures should correspond to $2[V]_T^{3+}2[V]_O^{2+}2[Fe]_O^{3+}$ and $2[Fe]_T^{2+}2[Fe]_O^{3+}2[V]_O^{3+}$, respectively. The formation energies, E_{spinel}, can be described with behind general Eq. (1).

$$E_{spinel} = E_{total} - (E_{[Fe,V]_T} + E_{[Fe,V]_O}) \quad \cdots\cdots\cdots (1)$$

Here, E_{total} is total energy of every spinel system, $E_{[Fe,V]T}$ and $E_{[Fe,V]O}$ indicates the energies of corresponding bivalent and trivalent oxides in tetrahedral and octahedral interstices, respectively. We have also employed different functionals to calculate formation energies in order to compare reliability of hybrid PBE0 functional (In **Table 3**, VBH: von Barth-Hedin,[16] PBE: Perdew-Burke-Ernzerhof,[17] B3LYP: Becke-Lee-Yang-Parr[18] and PBE0: 75% Perdew-Burke-Ernzerhof hybrid with 25% Hartree Fock.[19] The B3LYP, PBE and VBH functionals have suggested consistent trend of stability. The inverse FeV_2O_4 and VFe_2O_4 spinels are always more favorable. The PBE0 not only has reproduced qualitatively this trend, but also has behaved best on accuracy of energetics. The inverse VFe_2O_4 spinels are absolutely dominant in all spinels containing iron and vanadium, since the formation energies are lower significantly compared with other spinel structures. Furthermore, the slag oxides containing vanadium is produced in Fe-rich condition. As a result, we have decided to employ PBE0 functional to quantify fraction of two isomeric inverse spinels (F-I-1 and F-I-2) in equilibrium.

The energetic calculations of ground state with *ab initio* approaches are relevant for quantification at low temperature. In industrial process, the chemical reactions take place

around 1 700 K temperature. Therefore, thermal contributions are needed to be taken into account, *via* calculating lattice vibrations, on the basis of quantum mechanical scheme,[20] to calculate fraction of the two isomeric inverse spinels. The Gibbs free energies (Eq. (2)) were employed to discuss relative stability of F-I-1 and F-I-2 spinels.

$$G_T = E_{pot} + E_{ZPE} + H_T + pV - TS \quad \cdots\cdots\cdots (2)$$

Here, G_T is referred to Gibbs free energies at temperature T, E_{pot} is electronic potential, E_{ZPE} is zero point energies, and H_T is contributions from classical vibrational Hamiltonian. P, V, T, R and S indicate atmosphere pressure, volume, temperature, gas constant and entropy of F-I-1 and F-I-2 spinels. Born-Oppenheimer potential energy surface of a system with N atoms is a function of phase space with $3N$ coordinates. In the harmonic approximation, the classical vibrational Hamiltonian, H_T, of a polyatomic system takes following form including kinetic energy, K_T, and thermal vibrational potential, V_T, in terms of the weighted displacement coordinates x. The u denotes vibrational velocity of atoms in Eq. (3).[20]

$$H_T = K_T + V_T = \frac{1}{2}\left(\sum_i M_i u_i^2 + \sum_{ij} x_i H x_j\right) \quad \cdots\cdots (3)$$

The volumes of F-I-1 and F-I-2 spinels are comparable, so we have chosen constant standard atmosphere pressure in present work. The equilibrium constant $K_{a\to b}$ accounts for isomerization reaction from F-I-1 to F-I-2. Q_a and Q_b are partition function of isomeric F-I-1 and F-I-2. Because the chemical reactions take place at approximately 1 700 K, we have assumed activation energies of isomerization reactions are comparable; meanwhile, the chemical reactions can reach thermodynamic equilibrium. Then the probability of isomeric F-I-1 and F-I-2 can be characterized by statistical Boltzmann function and their fractions were evaluated with Eq. (6).[21]

$$\Delta G_{T,a\to b}^0 = -RT \ln K_{a\to b} \quad \cdots\cdots\cdots (4)$$

$$x_b = \frac{K_{a\to b}}{\sum_{b=a}^b K_{a\to b}} \quad \cdots\cdots\cdots (5)$$

$$x_a = \frac{Q_a \exp[-\Delta G_{0,a}^0/(RT)]}{\sum_{b=a}^b Q_b \exp[-\Delta G_{0,b}^0/(RT)]} \quad \cdots\cdots (6)$$

Although the Gibbs free energies difference of F-I-1 and F-I-2 are similar at 300 K and 1 700 K, the fraction of F-I-1 and F-I-2 is temperature dependent. Our calculations indicate entropy dependence plays a significant role in isomeric fraction at 1 700 K temperature, namely 96% and 4% (**Table 4**)

Table 3. Formation energies (E_{spinel}) of normal and inverse spinel structures were computed using Eq. (1) and compared with respect to four density functionals (eV/primitive cell).

Functionals	VBH	PBE	B3LYP	PBE0
V-N	1.47	0.54	1.70	2.53
V-I-1	1.38	0.29	0.37	0.71
V-I-2	1.45	0.27	0.37	0.71
F-N	2.46	1.21	4.12	4.67
F-I-1	0.31	−0.42	−1.42	−1.61
F-I-2	0.31	−0.42	−1.42	−1.61

Table 4. Calculated thermodynamic quantities of isomeric spinel structures, namely, F-I-1 and F-I-2, under standard atmosphere pressure condition, namely, 1 atm, and temperature at 300 K and 1 700 K, respectively.

1 700 K	S(J/mol·K)	ΔG(kJ/mol)	lnQ	x
F-I-1	678	−688	3.01E + 25	96%
F-I-2	655	−652	2.83E + 25	4%
300 K	S(J/mol·K)	ΔG(kJ/mol)	lnQ	x
F-I-1	173	−20	4.79E + 24	80%
F-I-2	154	−5	4.00E + 24	20%

for F-I-1 and F-I-2, respectively. However, the fraction of F-I-1 is only 80% at room temperature (300 K).

3.2. Theoretical Advices for Experiments

The realistic chemical reactions are always in nonequilibrium and quasiequilibrium. As a result, F-I-1 and F-I-2 can also possibly coexist with the other spinel structures in slag oxides containing vanadium. However, experimental characterization to justify normal and inverse spinels, on the basis of atomistic level diffraction, *e.g.* X-ray diffraction (XRD), is always difficult as their identical space group and similar crystal plane spacing. In other words, the experimental characterization is equivalent to justify cationic preference on tetrahedral and octahedral interstices. The different crystal field splitting of $3d$ orbitals for transition metal with different coordination is well-known. Thus, we have calculated L_2 and L_3-edges XANES spectra to evaluate tetrahedral Fe and V and octahedral Fe and V. The $2p$ orbitals are split by spin–orbit interaction into $2p_{1/2}$ and $2p_{3/2}$, namely L_2 and L_3, with the subscripts representing quantum number of total angular momentum. After absorbing phonon energies in the form of X-ray, an electron from the $2p$ level is excited into the t_{2g} or e_g states, and schematic diagram of this excitation is shown in **Fig. 2**. In this work, large clusters containing 448 atoms were used to simulate spinels, namely, $Fe_{64}V_{128}O_{256}$ for V-rich spinels and $V_{64}Fe_{128}O_{256}$ for Fe-rich ones, to ensure reliable computed spectra.

The computed L_3 and L_2-edges XANES spectra of Fe cations are shown in **Fig. 3**(a). The $2p$ orbitals splitting, around 11.6 eV, agree with experimental observations of Fe_2O_3 nanowires and powders,[22] namely 12.6–13.0 eV. The slight estimations, namely 1.0–1.4 eV, are most likely due to modeling realistic spinels as cluster and using LDA functional in FEFF9.0 code. Chemical shift of white line at L_3 and L_2-edges, approximately 1 eV, goes from tetrahedral Fe cations to octahedral ones. In experiment, the observed chemical shift was 1.8 eV, comparing Fe_2CO_3 with Fe_2O_3.[23] On the other hand, Benzerara *et al.*[24] had also obtained a chemical shift of 1.7 eV from pyroxene (Fe^{2+}) to Fe_2O_3. Both Fe in pyroxene and Fe_2CO_3 are octahedral coordinated, where electronic screening effects differ with tetrahedral Fe^{2+} in
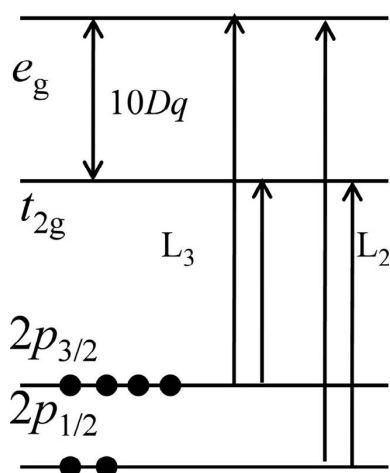
spinel structures. So it can explain a smaller chemical shift in spinels.

Furthermore, we also need to find difference of tetrahedral and octahedral V cations. We have reproduced XANES spectra of V_2O_3 measured by Park *et al.*[25] and calculated by Brik *et al.*[26] The computed spin-orbit splitting of V $2p$ is around 8.6 eV, in comparison with observed 8 eV in experiment.[25] The intensive $3d$ orbitals splitting of octahedral V cations were also observed in this work. The bifurcate absorption peaks can explain threefold degenerated t_{2g} level and twofold e_g level, while $3d$ orbitals splitting of tetrahedral V cations obviously favor smaller energies with a single broaden absorption peak. This important electronic information can advise experimental work to study V cationic interstices distribution. According to above discussion, electronic spectra are quite relevant than atomistic level diffractions for quantifying solid solution. We thus advise approaches combined atomistic level diffraction and electronic level absorption spectra, *e.g.* XRD and XANES or electron loss near edge structure (ELNES), measurements to investigate cationic interstices preference. Recently, Gomes *et al.* have employed combined XRD and XANES to address successfully cation redistribution of zinc ferrite.[27] Akhtar *et al.* had also characterized structure, valence states and cationic occupation of Sr–Fe–O solid solutions using combined XRD and XANES measurements.[28]
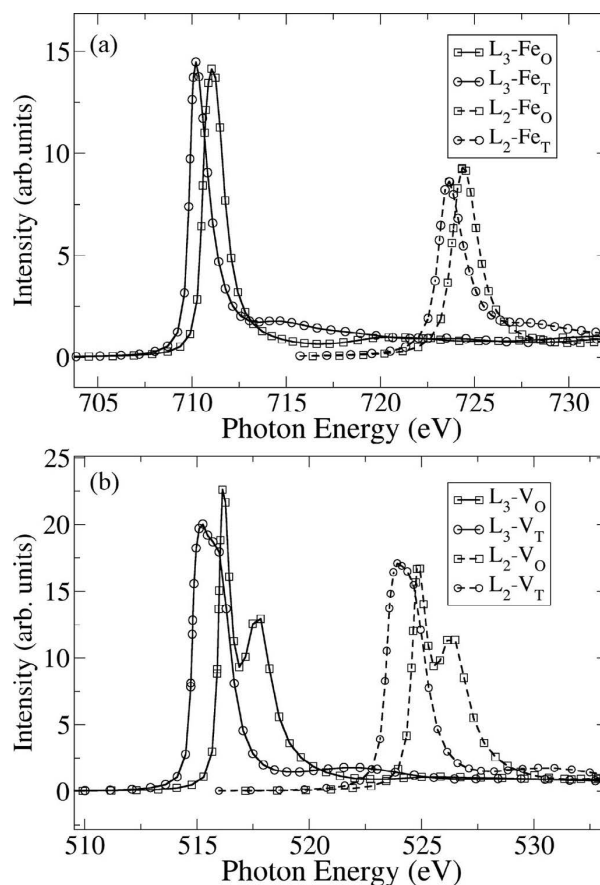
Fig. 3. Computed L_3 and L_2 edges XANES of (a) tetrahedral Fe cations and octahedral Fe cations, (b) tetrahedral V cations and octahedral V cations in all studied spinel structures. The subscripts T and O indicate tetrahedral and octahedral interstices, respectively.

Fig. 2. One-electron transition is represented schematically for L_2 and L_3 absorption bands in the XANES spectra.

4. Conclusions

In summary, we have performed *ab initio* calculations to address normal and reverse spinels containing iron and vanadium. The Mulliken charges indicate valence state of tetrahedral Fe and V cations is bivalent in Fe-rich condition, while octahedral Fe and V prefer trivalence. In V rich condition, Fe valence states in tetrahedral and octahedral interstices are the same as those in Fe rich cases. However, the V cations have contrary valence states, namely, V^{3+}, in tetrahedral interstices, and mixed valence states in octahedral sites. According to computed formation energies, the vanadium-iron spinels are most likely to present as inverse configurations. The fractions of two inverse spinels in Fe-rich condition at room temperature (300 K) are 80% and 20%, respectively. For spinels containing iron and vanadium, the chemical shift of white lines for Fe^{2+} and Fe^{3+} cations is around 1 eV. The 3d orbital splitting of octahedral V cations is much stronger than tetrahedral V cations.

REFERENCES

1) J. Diao, B. Xie, C. Q. Ji, X. Guo, Y. H. Wang and X. J. Li: *Cryst. Res. Technol.*, **44** (2009), 707.
2) X. S. Li, B. Xie, G. E. Wang and X. J. Li: *Trans. Nonferrous Met. Soc. China*, **21** (2011), 1860.
3) V. Nivoix and B. Gillot: *Chem. Mater.*, **12** (2000), 2971.
4) B. Gillot and M. Nohair: *Phys. Stat. Sol. (A)*, **148** (1995), 239.
5) A. S. Radtke: *Am. Mineral.*, **47** (1962), 1284.
6) B. Reuter, E. Riedel, P. Hug, D. Arndt, U. Geisler and J. Behnke: *Z. Anorg. Allg. Chem.*, **369** (1969), 306.
7) S. H. Chung, H. P. HA, W. S. Jung and J. Y. Byun: *ISIJ Int.*, **46** (2006), 1523.
8) R. I. L. Guthrie, M. Isac and D. Li: *ISIJ Int.*, **50** (2010), 1805.
9) W. K. Li, G. D. Zhou and T. C. W. Mak: Advanced Structural Inorganic Chemistry, Oxford University Press, New York, (2008).
10) R. Dovesi, V. R. Saunders, C. Roetti, R. Orlando, C. M. Zicovich-Wilson, F. Pascale, B. Civalleri, K. Doll, N. M. Harrison, I. J. Bush, Ph. D'Arco and M. Llunell: CRYSTAL09, User's Manual, University of Torino, Torino, (2009).
11) H. J. Monkhorst and J. D. Pack: *Phys. Rev. B*, **13** (1976), 5188.
12) G. Valerio, M. Catti, R. Dovesi and R. Orlando: *Phys. Rev. B*, **52** (1995), 2422.
13) W. C. Mackrodt, N. M. Harrison, V. R. Saunders, N. L. Allan, M. D. Towler, E. Apra and R. Dovesi: *Philos. Mag. A*, **68** (1993), 653.
14) M. Corno, C. Busco, B. Civalleri and P. Ugliengo: *Phys. Chem. Chem. Phys.*, **8** (2006), 2464.
15) A. L. Ankudinov, B. Ravel, J. J. Rehr and S. D. Conradson: *Phys. Rev. B*, **58** (1998), 7565.
16) U. von Barth and L. Hedin: *J. Phys. C: Solid State Phys.*, **5** (1972), 1629.
17) J. P. Perdew, K. Burke and M. Ernzerhof: *Phys. Rev. Lett.*, **77** (1996), 3865.
18) A. D. Becke: *J. Chem. Phys.*, **98** (1993), 5648.
19) J. Perdew, M. Ernzerhof and K. Burke: *J. Chem. Phys.*, **105** (1996), 9982.
20) F. Pascale, C. M. Zicovich-Wilson, F. Lopez, B. Civalleri, R. Orlando and R. Dovesi: *J. Comput. Chem.*, **25** (2004), 888.
21) Z. Slanina, F. Uhlik, S. L. Lee, L. Adamowicz and S. Nagase: *Int. J. Quantum Chem.*, **108** (2008), 2636.
22) Y. C. Lee, Y. L. Chueh, C. H. Hsieh, M. T. Chang, L. J. Chou, Z. L. Wang, Y. W. Lan, C. D. Chen, H. Kurata and S. Isoda: *Small*, **3** (2007), 1356.
23) A. Isambert, T. De Resseguier, A. Gloter, B. Reynard, F. Guyot and J. P. Valet: *Earth Planetary Sci. Lett.*, **243** (2006), 820.
24) K. Benzerara, T. H. Yoon, N. Menguy, T. Tyliszczak and G. E. Brown, Jr.: *Proc. Natl. Acad. Sci. USA*, **102** (2005), 979.
25) J. H. Park, L. H. Tjeng, A. Tanaka, J. W. Allen, C. T. Chen, P. Metcalf, J. M. Honig, F. M. F. de Groot and G. A. Sawatzky: *Phys. Rev. B*, **61** (2000), 11506.
26) M. G. Brik, K. Ogasawara, T. Ishii, H. Ikeno and I. Tanaka: *Radiat. Phys. Chem.*, **75** (2006), 1564.
27) J. A. Gomes, G. M. Azevedo, J. Depeyrot, J. Mestnik-Filho, G. J. da Silva, F. A. Tourinho and R. Perzynski: *J. Mag. Mag. Mater.*, **323** (2011), 1203.
28) M. Javed Akhtar and R. Tahir Ali Khan: *Mater. Charact.*, **62** (2011), 1016.